RESEARCH ARTICLE
SOLID EARTH: TECTONOPHYSICS

Earth and Planetary Physics
2: 67–73, 2018
doi: 10.26464/epp2018006

Different earthquake patterns for two neighboring fault segments within the Haiyuan Fault zone

ZhiKun Ren[1,2*], ZhuQi Zhang[1], and PeiZhen Zhang[1,3]

[1]State Key Laboratory of Earthquake Dynamics, Institute of Geology, China Earthquake Administration, Beijing 100029, China;

[2]Key Laboratory of Active Tectonics and Volcanos, Institute of Geology,China Earthquake Administration, Beijing 100029, China;

[3]School of Earth Science and Geological Engineering, Sun Yat-Sen University, Guangzhou 510275, China

Abstract: Characteristic slip and characteristic earthquake models have been proposed for several decades. Such models have been supported recently by high-resolution offset measurements. These models suggest that slip along a fault recurs via similarly sized, large earthquakes. The inter-event strain accumulation rate (ratio of earthquake slip and preceding interseismic time period) is used here to test the characteristic earthquake model by linking the slip and timing of past earthquakes on the Haiyuan Fault. We address how the inter-event strain accumulation rate varies over multiple seismic cycles by combining paleoearthquake studies with high-resolution airborne light detection and ranging (LiDAR) data to document the timing and size of paleoearthquake displacements along the western and middle segments of the Haiyuan Fault. Our observations encompass 5 earthquake cycles. We find significant variations over time and space along the Haiyuan Fault. We observe that on the middle segment of the Haiyuan Fault the rates slow down or increase as an anti-correlated function of the rates of preceding earthquakes. Here, we propose that the inter-event strain accumulation rates on the middle segment of the Haiyuan Fault are oscillating both spatially and temporally. However, along the western segment, the inter-event strain accumulation rate is both spatially and temporally steady, which is in agreement with quasi-periodic and slip-predictable models. Finally, we propose that different fault segments within a single fault zone may behave according to different earthquake models.

Keywords: Haiyuan Fault; LiDAR; inter-event strain accumulation rates variation; earthquake model

Citation: Ren, Z. K., Zhang, Z. Q., and Zhang, P. Z. (2018). Different earthquake patterns for two neighboring fault segments within the Haiyuan Fault zone. *Earth Planet. Phys.*, *2*, 67–73. http://doi.org/10.26464/epp2018006

1. Introduction

It is rare that field observations are sufficient to document both the timing and amount of seismic slip in repeated earthquakes along an individual fault (Akçiz et al., 2014; Ludwig et al., 2010; Weldon et al., 2004; Zielke et al., 2010). However, since the 1980s various models for earthquake recurrence patterns have been proposed (Schwartz and Coppersmith, 1984; Shimazaki and Nakata, 1980), among which the simplest are characteristic slip and characteristic earthquake models, though these are patterns that have rarely been verified by observation (Klinger et al., 2011). The pattern of strain accumulation during the inter-seismic period is still unknown, yet in testing earthquake recurrent models, strain accumulation has been assumed to be proportional (Murray and Segall, 2002; Segall and Harris, 1987) ; this assumption is a key issue in assessing the probably time of future large earthquakes (Fialko, 2006; Murray and Segall, 2002). Previous studies have attempted to estimate the strain rate along active faults, using GPS, InSAR (Interferometric Synthetic Aperture Radar) as well as geological data (Feldl and Bilham, 2006; Fialko, 2006; Fialko et al., 2005; Mazzotti et al., 2011; Murray and Segall, 2002; Smalley et al., 2005). Unfortunately, GPS and InSAR methods provide current strain rates over only the several tens of years since the deployment of the GPS stations and the launching of the InSAR satellite; there has not been enough time to reveal the strain rate status over multiple seismic cycles. Precise, spatially dense measurements of surface deformation through time would greatly improve chances of assessing different scenarios of inter-event strain accumulation rates and thus improve the likelihood of predicting future large earthquakes. Here, along a portion of the 1920 Haiyuan earthquake rupture (Figure 1), we combine a collection of previous paleoearthquake studies (IGCEA and NSBCEA, 1990; Liu B et al., 1995; Min W et al., 2001; Ran YK et al., 1997; Zhang PZ et al., 1988b, 2005) with analysis of high-resolution airborne light detection and ranging (LiDAR) data (Ren ZK et al., 2016) to document both the timing and displacement of the last five earthquakes that have occurred along the western and middle segments of the Haiyuan Fault, respectively. Below, we first present the data on which our estimates of inter-event strain accumulation rates are constructed. Under the assumption that the measured offset carries the inter-event strain accumulation information of the past earthquakes, we calculate the inter-event strain accumulation rates of the past five earthquakes along the western and middle segments of the Haiyuan Fault, respectively. Finally, we propose two different earthquake models according to the variation of inter-event strain accumulation rate for the two fault segments within the Haiyuan

Correspondence to: Z. K. Ren, rzk@ies.ac.cn; Lzkren@gmail.com
Received 11 OCT 2017; Accepted 19 DEC 2017.
Accepted article online 26 DEC 2017.

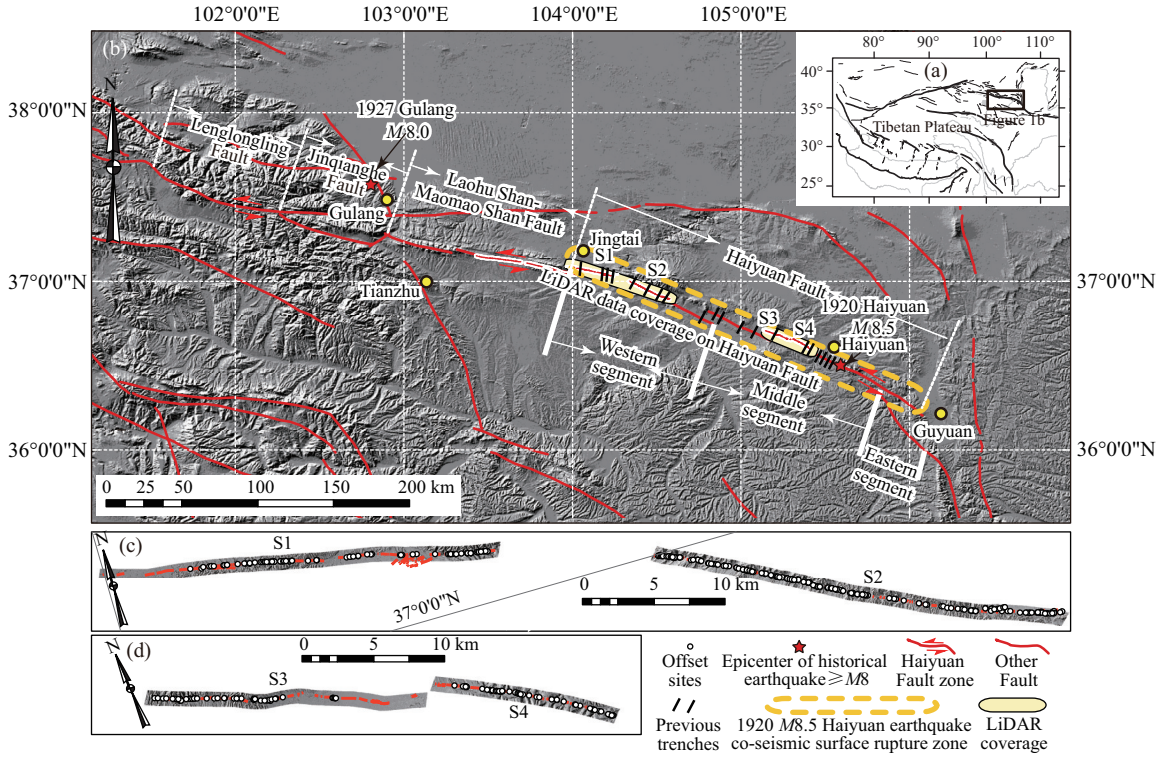

Figure 1. (a) Simplified tectonic map of Tibetan Plateau; (b) Tectonic and geomorphic map of the Haiyuan Fault zone; (c) Airborne LiDAR data coverage of segments S1–S2; (d) Airborne LiDAR data coverage of segments S3–S4. The yellow dashed rectangle indicates the region that coseismically ruptured during the 1920 *M*8.5 earthquake. The white circles represent the offset sites.

Fault zone.

2. Geological Setting

The Haiyuan Fault is a major left-lateral strike-slip fault in northeastern Tibet (Figure 1). Previous researchers (Burchfiel et al., 1991) suggested that the Haiyuan Fault experienced thrusting in the Pliocene, caused by northeastward expansion of the Tibetan Plateau. Its sense of motion changed in the late Pliocene or early Pleistocene to the current, dominantly left-lateral strike slip sense of motion (Burchfiel et al., 1991). Fault slip rates along the Haiyuan Fault have been constrained by a number of studies that utilized geologic (Lasserre et al., 1999; Li CY et al., 2009; Zhang PZ et al., 1988a), geodetic (Wang M et al., 2003; Zhang PZ et al., 2004), and InSAR data (Cavalié et al., 2008; Jolivet et al., 2012; Li YC et al., 2016). The geological slip rate is now widely accepted to be 4.5±1.0 mm/a along the western and middle segments of the Haiyuan Fault (Li CY et al., 2009).

The Haiyuan Fault has been the site of numerous paleoseismic trenching studies since the 1980s (IGCEA and NSBCEA, 1990; Liu B et al., 1995; Min W et al., 2001; Ran YK et al., 1997; Zhang PZ et al., 1988b, 2005). Most trenches are located along the western and middle segments of the fault (Figure 1). The results of these studies are summarized in the form of a space-time diagram (Ren ZK et al., 2016). The temporal limits are estimated to constrain the age of paleo-earthquakes at each trench. The limits are then correlated among adjacent trenches to evaluate the spatial extent and timing of paleo-earthquakes along the western and middle segments of the fault. The recorded paleo-earthquakes can be traced back about 11000 years. The correlated records reveal that five earthquakes have occurred on both the western and middle segments of the Haiyuan Fault in the most recent ~6500 years, though the timing of individual events on the two segments is somewhat different. The paleoseismic investigations along the 1920 rupture trace show that the recurrence interval of earthquakes of similar size to the 1920 event is on the order of ~1000 years (IGCEA and NSBCEA, 1990; Liu B et al., 1995; Min W et al., 2001; Ran YK et al., 1997; Zhang PZ et al., 1988b, 2005).

3. Methods

3.1 Introduction to Previous Offset Measurements

Airborne LiDAR data along the Haiyuan Fault were collected in November 2011. Details of the data collection and preparation are reported by Ren ZK et al. (2016). The resulting digital elevation model enabled Ren ZK et al. (2016) to identify and measure 320 left-lateral offsets of geomorphic and cultural features such as gullies, terrace risers, and man-made stone walls. Measurements utilized the method of Zielke et al. (Zielke et al., 2010, 2012) using LaDiCaoz—a MATLAB program. Offsets interpreted to be the result of one or more earthquakes along the fault are measured by back-shift, stretching and matching the topographic profile perpendicular to the channels and parallel to the faults on both sides of the fault. In this manner, the best offset values are obtained semi-automatically from LaDiCaoz by fitting the topographic profiles.

In our previous study (Ren ZK et al., 2016), we obtained 320 offset measurements from the 88 km distance of the Haiyuan Fault covered by the LiDAR survey. The quality of our previous measurements follows five ranks with corresponding weight factors: high=1.0; high-moderate=0.75; moderate=0.5; moderate-low=0.25 and low =0.0 (Zielke et al., 2010). The *cumulative offset probability density* (COPD) values are used to group the offset (Ren ZK et al., 2016). Our synthesis of previous observations reveals that the largest cumulative offsets preserved along the fault reach up to 30 meters (Figure 2).

The COPD plot shows five distinctive groups/clusters of accumulated slip. For the purpose of this study we assume that these five clusters represent the offset of the five most recent paleo-events/earthquakes (Figure 2) (Ren ZK et al., 2016).

Based on this assumption, we are able to determine the average offset of the five most recent earthquakes along the western and middle Haiyuan Fault, as identified in the aforementioned paleoseismic excavations (IGCEA and NSBCEA, 1990; Liu B et al., 1995; Min W et al., 2001; Ran YK et al., 1997; Zhang PZ et al., 1988b, 2005).

3.2 New Methods to Interpret Previous Offset Data

The displacement for individual clusters is interpreted as the difference in the cumulative offsets between sequentially adjacent paleo-events (Figure 2b). In order to better evaluate the slip-releasing history of past events, we need to estimate the coseismic offsets of each earthquake.

On the Haiyuan Fault, paleo-earthquakes are identified/derived from stratigraphic record by correlating faulting evidences from multiple trenches that cover a total distance of ~150 km along the fault. Hence, individual earthquakes that can be identified in (all) those trenches (hence exhibiting a rupture length above 150km) must be of significant size (Wells and Coppersmith, 1994). Consequently, we consider it plausible to correlate stratigraphic evidence of faulting (from paleoseismic excavations) directly with the observed offset clusters.

Since the offset measurements are not at the same sites, we begin by averaging the offset data using distance windows of 1-km, 2-km and 5-km, respectively. Among these, the 1-km window is closest to the real offset value, which could show both local (maybe related to fault structure) and regional (maybe related to earthquake pattern) offset variations. To obtain the offset of each earthquake, we need to subtract the co-seismic offset of the younger earthquake from the cumulated offsets of multiple earthquakes. However, only the co-seismic offset of the 1920 Haiyuan earthquake is directly measured. In this study, we first subtract the co-seismic offset of the 1920 Haiyuan earthquake from the averaged offset of the events I and II derived from the windowing approach. Then, we subtract the measured cumulative offset of event I and II from the averaged cumulative offset of the events I, II and III, and so on. Consequently, the coseismic offset distributions of five events were obtained (Figure 2b). Coseismic displacements average ~5 m and vary by a factor of up to two from event to event.

4. Results

The division of the seismic offset of each paleo-event by the preceding inter-event time interval provides an estimate of inter-event strain accumulation rate for each of the 5 identified earthquakes along the western and middle sections of the Haiyuan Fault (Figure 2b), following the aforementioned assumption of a direct relationship between stratigraphic and geomorphic earthquake evidence. The inter-event strain accumulation rates are generally between 3 and 5 mm/a on the western segment but span a much larger interval, from 3 to 15 mm/a, on the middle segment. The estimated inter-event strain accumulation rates also vary along strike for given individual events. For example, the inter-event strain accumulation rate after event IV on the western segment (WIV) decreases from S1–S2 to S3–S4 (Figure 3). From the western to the middle segments, the rates show a spatial variation of a factor of three. The comparisons of inter-event strain accumulation rates are shown in Figure 3; the inter-event strain accumulation rate is roughly stable (range from 3–5mm/a) on segment S2 (Figures 3a-3d), but relatively oscillate (range from 3–15 mm/a) on segments S1, S3 and S4 (Figures 3a-3d). The most obvious variation in inter-event strain accumulation is observed from events II, III, IV and V on segments S3–S4. The rates first decrease from ~15 mm/a (Event V) to ~3 mm/a (Event IV), then increase to ~10 mm/a (Event III) and finally decrease to ~5 mm/a (Event II) (Figures 3b-3d).

5. Discussion

The varying inter-event strain accumulation rates may reflect perturbations to the mechanical properties of ruptured faults during past earthquakes, such as the frictional features of the fault zone, and asperities on the fault plane. The observed variation over time and along fault strike suggests that inter-event strain accumulation for strong earthquake is neither spatially nor temporally constant across the entire Haiyuan Fault.

On the Haiyuan Fault, the inter-event strain accumulation rates show a spatial variation from 3 mm/a to15 mm/a between middle and western segments. There are three possible explanations for the spatial variations. The first one: a spatially constant strain accumulation rate may nevertheless result in variations in the inter-event strain accumulation rate because of incomplete coseismic strain release, i.e., slip, along a fault (Chéry and Vernant, 2006; Weldon et al., 2004, 2005). We speculate that incomplete coseismic strain release may lead to an oscillatory behavior, where a relatively small slip event tends to be followed by relatively larger slip events.

The second explanation is the inverse of the first: the accumulated strain may be completely released during strong earthquakes but the inter-event strain accumulation may not be spatially constant. The inter-event strain accumulation rate is spatially and temporally variable and, thus, so is the coseismic strain release because the release is complete from one event to the next. Consequently, the higher inter-event strain accumulation rates on segments S3–S4 may indicate that the middle segment of the Haiyuan Fault has accumulated strain at a higher rate than the western segment. Hence, the slip rate of the Haiyuan Fault might not be uniform along the segments S1–S2 and S3–S4.

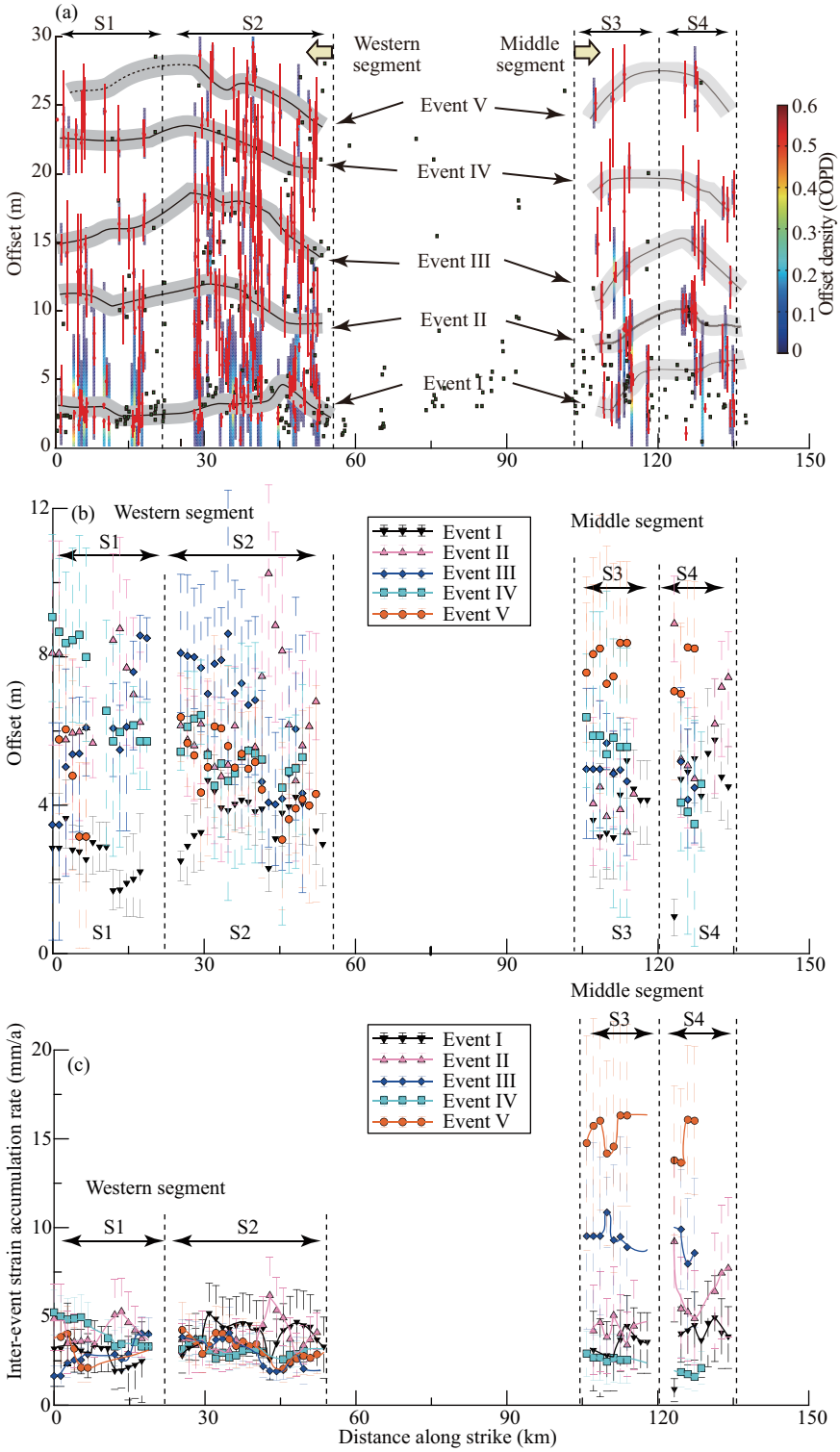

Figure 2. (a) The offset and normalized COPD distribution measured from the airborne LiDAR data along the Haiyuan Fault zone, and the corresponding five events deduced from the COPD distribution. The color bar shows the value of the COPD. The red dots represents the offset measured in this study, the green dots show the offset measured in field by Deng et al. (Deng QD et al., 1986) (Modified from (Ren ZK et al., 2016)). The derived coseismic offset (b) and the inter-event strain accumulation rates (c) of event I, II, III, IV and V. The average releasing rate over multiple seismic cycles derived from geological offset and corresponding paleoseismic data along the Haiyuan Fault. The timing of each event is from the paleoseismic data (IGCEA and NSBCEA, 1990; Liu B et al., 1995; Min W et al., 2001; Ran YK et al., 1997; Zhang PZ et al., 1988b, 2005). The black triangles, pink triangles, blue diamonds, light blue rectangles and orange dots represent the accumulation rates for the five earthquakes corresponding to the offset clusters, among which, the black triangles indicate the most recent one—the 1920 Haiyuan earthquake. Dashed lines show the errors.

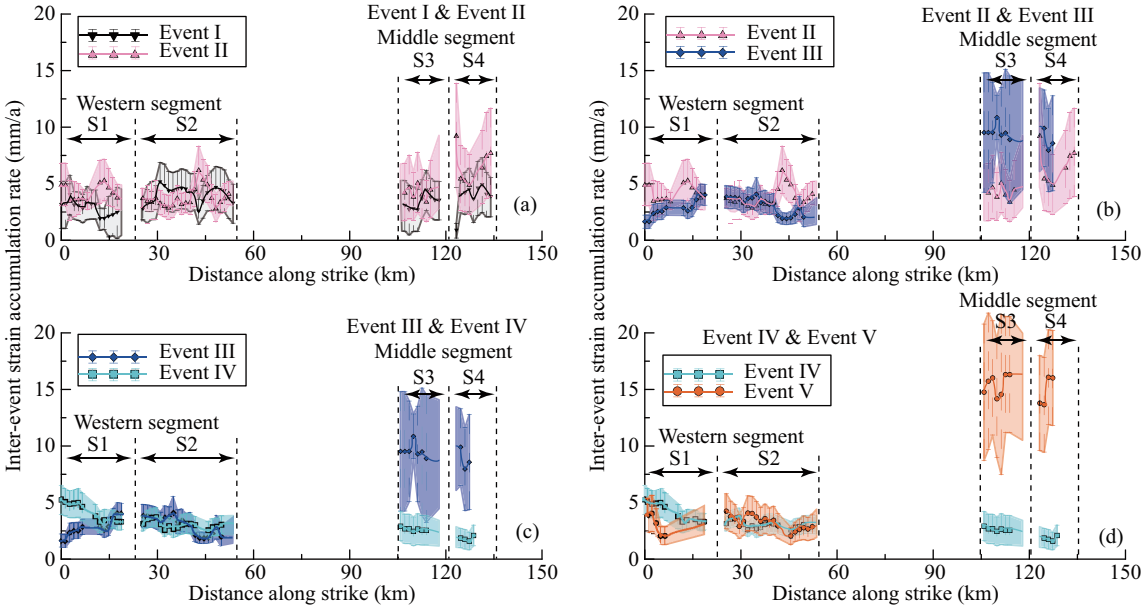

Figure 3. The inter-event strain accumulation rate variation between each successive two events. The inter-event strain accumulation rate variations between events I and II (a), events II and III (b), events III and IV (c), events IV and V (d). Thick colored lines and polygons show the inter-event strain accumulation rate for event I (black), event II (pink), event III (blue), event IV (light blue), and event V (orange).

The third possibility is that the strain accumulation rate varies but, in addition, its release is not incomplete; if so, the spatial variation is meaningless, i.e., the rupture pattern on the Haiyuan Fault cannot be discovered using slip and time information of past earthquakes.

Our results suggest that, in general, the inter-event strain accumulation rate on the Haiyuan Fault varies through time. There is an anti-correlation between each two successive events on segments S3–S4 (Figure 3), which might be related with previous deficits or surpluses of slip on the fault. This finding indicates that the occurrence of past strong earthquakes and consequent post-seismic status of the fault zone will affect the slip in the next earthquake. For example, if the slip for the previous earthquake is low, then we predict that slip will be higher in the next event, and vice visa, which has also been found in inversion studies of the slip balance during the seismic cycle (Wang LF et al., 2015, 2017).

Our observations indicate that inter-event strain accumulation on fault segments S1–S2 are low when accumulation rates are relatively high on segments S3–S4 (Figure 3). Temporal variations may suggest that the high accumulation rates for events III and V are due to the low accumulation rates for events II and IV, respectively. Overall, our findings indicate the inter-event strain accumulation rates are both spatially and temporally varying on the middle segment of the Haiyuan Fault, which might reveal a kind of rupture pattern. However, along the western segment, the inter-event strain accumulation rate is relatively stable (Figure 4).

According to characteristic earthquake models, the inter-event strain accumulation rates should be both spatial and temporally constant. In a characteristic slip model, inter-event strain accumulation rates should be spatially constant along fault segments and temporally variable between earthquakes. By illustrating the average co-seismic slip and corresponding ages, we were able to find that the earthquake recurrence behavior differs for the western and middle segments (Figure 4). The earthquake recurrence pattern on the western segment is quasi-periodic (Scharer et al., 2010) and appears to follow a slip-predictable model (Shimazaki and Nakata, 1980). However, the earthquake recurrence pattern on the middle segment is more random, and does not conform to characteristic, slip-predictable, or time-predictable models

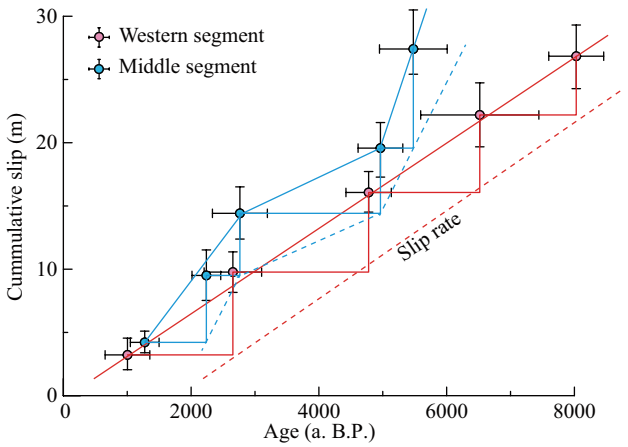

Figure 4. The plots show the cumulative offsets and corresponding ages of the five events (from young to old) on western and middle segments. Red lines show the results of western segment and blue curves show the results of middles segment. The red lines indicate the earthquake recurrence pattern on western segment is quasi-periodic, following slip-predictable (upper bound) and time-predictable models (lower bound), which roughly following characteristic earthquake model. The blue lines indicate earthquake recurrence pattern one middle segment is chaotic, neither following slip-predictable nor time-predictable models.

(Schwartz and Coppersmith, 1984; Shimazaki and Nakata, 1980). Hence, our finding suggest that the earthquake recurrence behavior varies for different segments even within a single fault zone.

6. Conclusions

We analyzed the inter-event strain accumulation history of past five earthquake cycles on the Haiyuan Fault using combined paleoseismic and offset data derived from airborne LiDAR data. By using coseismic offset and corresponding accumulation times of each event, we obtained the inter-event strain accumulation rates for each event. The rates are relatively constant at ~3–5 mm/a on the western segment but range from ~3–5 mm/a to ~10–15 mm/a along the middle segment. The earthquake recurrence pattern is quasi-periodic on the western segment, consistent with slip-predictable model; on the middle segment of the Haiyuan Fault, however, the observed pattern agrees better with random slip variable models. It is not advisable to extrapolate these observations as predicting more or less hazard on various fault segments, because we do not know how big the tectonic store of strain may be (one could get two large events followed by a smaller one, for example); a 3 m slip may be just as destructive as a 6 m slip along a given segment of fault. Finally, we propose that different earthquake models may be appropriate for the western and middle segments within the Haiyuan Fault zone, a finding that might shed new light on past and future earthquake pattern studies.

Acknowledgements

We appreciate S. G. Wesnousky for his help in improving both the scientific content and the English of an early version of this report. Thanks are also due to R. Arrowsmith and O. Zielke for sharing the offset measurement program LaDiCao program based on MATLAB (MATrix LABoratory) programming language. We appreciate the critical review of three anonymous reviewers and thank Editor Wei Leng and Sufang Hu for handling the manuscript. This work was supported by the NSFC (41472201, 41304073, 41661134011, and 41761144071) and the Stake Key Laboratory of Earthquake Dynamics (SKLED, LED2014A03). Original LiDAR data are collected by Institute of Geology, China Earthquake Administration.

References

Akçiz, S. O., Ludwig, L. G., Zielke, O., and Arrowsmith, J. R. (2014). Three-dimensional investigation of a 5 m deflected swale along the San Andreas fault in the Carrizo Plain. *Bull. Seism. Soc. Am.*, *104*(6), 2799–2808. https://doi.org/10.1785/0120120172

Burchfiel, B. C., Zhang, P. Z., Wang, Y. P., Zhang, W. Q., Song, F. M., Deng, Q. D., Molnar, P., and Royden, L. (1991). Geology of the Haiyuan Fault zone, Ningxia-Hui Autonomous Region, China, and its relation to the evolution of the Northeastern Margin of the Tibetan Plateau. *Tectonics*, *10*(6), 1091–1110. https://doi.org/10.1029/90TC02685

Cavalié, O., Lasserre, C., Doin, M.-P., Peltzer, G., Sun, J., Xu, X., and Shen, Z.-K. (2008). Measurement of interseismic strain across the Haiyuan Fault (Gansu, China), by InSAR. *Earth Planet. Sci. Lett.*, *275*(3-4), 246–257. https://doi.org/10.1016/j.epsl.2008.07.057

Chéry, J., and Vernant, P. (2006). Lithospheric elasticity promotes episodic fault activity. *Earth Planet. Sci. Lett.*, *243*(1-2), 211–217. https://doi.org/10.1016/j.epsl.2005.12.014

Deng, Q. D., Chen, S. F., Song, G. N., Zhu, S. L., Wang, Y. P., Zhang, W. Q., Jiao, D. C., Burchfiel, B. C., Molnar, P., … Zhang, P. Z. (1986). Variations in the geometry and amount of slip on the Haiyuan (Nanxihuashan) Fault zone, China and the surface rupture of the 1920 Haiyuan earthquake. In S. Das, et al. (Eds.), *Earthquake Source Mechanics* (pp. 169–182). Washington, DC: American Geophysical Union. https://doi.org/10.1029/GM037p0169

Feldl, N., and Bilham, R. (2006). Great Himalayan earthquakes and the Tibetan plateau. *Nature*, *444*(7116), 165–170. https://doi.org/10.1038/nature05199

Fialko, Y., Sandwell, D., Simons, M., and Rosen, P. (2005). Three-dimensional deformation caused by the Bam, Iran, earthquake and the origin of shallow slip deficit. *Nature*, *435*(7040), 295–299. https://doi.org/10.1038/nature03425

Fialko, Y. (2006). Interseismic strain accumulation and the earthquake potential on the southern San Andreas fault system. *Nature*, *441*(7096), 968–971. https://doi.org/10.1038/nature04797

Jolivet, R., Lasserre, C., Doin, M.-P., Guillaso, S., Peltzer, G., Dailu, R., Sun, J., Shen, Z.-K., and Xu, X. (2012). Shallow creep on the Haiyuan Fault (Gansu, China) revealed by SAR Interferometry. *J. Geophys. Res.*: *Solid Earth*, *117*(B6). https://doi.org/10.1029/2011JB008732

Klinger, Y., Etchebes, M., Tapponnier, P., and Narteau, C. (2011). Characteristic slip for five great earthquakes along the Fuyun fault in China. *Nat. Geosci.*, *4*(6), 389–392. https://doi.org/10.1038/ngeo1158

Lasserre, C., Morel, P.-H., Gaudemer, Y., Tapponnier, P., Ryerson, F. J., King, G. C. P., Métivier, F., Kasser, M., Kashgarian, M., … Yuan, D. Y. (1999). Postglacial left slip rate and past occurrence of $M \geq 8$ earthquakes on the Western Haiyuan Fault, Gansu, China. *J. Geophys. Res.*: *Solid Earth*, *104*(B8), 17633–17651. https://doi.org/10.1029/1998JB900082

Li, C. Y., Zhang, P.-Z., Yin, J. H., and Min, W. (2009). Late Quaternary left-lateral slip rate of the Haiyuan Fault, northeastern margin of the Tibetan Plateau. *Tectonics*, *28*(5). https://doi.org/10.1029/2008TC002302

Li, Y. C., Shan, X. J., Qu, C. Y., and Wang, Z. J. (2016). Fault locking and slip rate deficit of the Haiyuan-Liupanshan fault zone in the northeastern margin of the Tibetan Plateau. *J. Geodynam.*, *102*, 47–57. https://doi.org/10.1016/j.jog.2016.07.005

Liu, B. (1995). *1:50, 000 Geological Map of the Eastern Segment of the Active Qilianshan Fault* (*Laohushan*, *Maomaoshan and Jinqianghe Fault*) (in Chinese). Beijing: Seismological Publishing House.

Ludwig, L.G., Akçiz, S.O., Noriega, G. R., Zielke, O., and Arrowsmith, J. R. (2010). Climate-Modulated Channel Incision and Rupture History of the San Andreas Fault in the Carrizo Plain. *Science*, *327*(5969), 1117–1119. https://doi.org/10.1126/science.1182837

Mazzotti, S., Leonard, L. J., Cassidy, J. F., Rogers, G. C., and Halchuk, S. (2011). Seismic hazard in western Canada from GPS strain rates versus earthquake catalog. *J. Geophys. Res.*: *Solid Earth*, *116*(B12), B12310. https://doi.org/10.1029/2011jb008213

Min, W., Zhang, P. Z., Deng, Q. D., and Mao, F. Y. (2001). Detailed study of Holocene paleoearthquakes of the Haiyuan active fault. *Geol. Rev.* (*in Chinese*), *47*(1), 75–81.

Murray, J., and Segall, P. (2002). Testing time-predictable earthquake recurrence by direct measurement of strain accumulation and release. *Nature*, *419*(6904), 287–291. https://doi.org/10.1038/nature00984

Ran, Y. K., Duan, R. T., Deng, Q. D., Jiao, D. C., and Min, W. (1997). 3-D trench excavation and paleoseismology at Gaowanzi of the Haiyuan Fault. *Seism. Geol.* (*in Chinese*), *19*(2), 97–107.

Ren, Z. K., Zhang, Z. Q., Chen, T., Yan, S. L., Yin, J. H., Zhang, P. Z., Zheng, W. J., Zhang, H. P., and Li, C. Y. (2016). Clustering of offsets on the Haiyuan Fault and their relationship to paleoearthquakes. *Geol. Soc. Am. Bull.*, *128*(1-2), 3–18. https://doi.org/10.1130/B31155.1

Scharer, K. M., Biasi, G. P., Weldon, R. J., and Fumal, T. E. (2010). Quasi-periodic recurrence of large earthquakes on the southern San Andreas fault. *Geology*, *38*(6), 555–558. https://doi.org/10.1130/g30746.1

Schwartz, D. P., and Coppersmith, K. J. (1984). Fault behavior and characteristic earthquakes: Examples from the Wasatch and San Andreas Fault Zones. *J. Geophys. Res.*: *Solid Earth*, *89*(B7), 5681–5698. https://doi.org/10.1029/JB089iB07p05681

Segall, P., and Harris, R. (1987). Earthquake deformation cycle on the San Andreas Fault near Parkfield, California. *J. Geophys. Res.*: *Solid Earth*, *92*(B10),

10511–10525. https://doi.org/10.1029/JB092iB10p10511

Shimazaki, K., and Nakata, T. (1980). Time-predictable recurrence model for large earthquakes. *Geophys. Res. Lett.*, *7*(4), 279–282. https://doi.org/10.1029/GL007i004p00279

Smalley, R., Ellis, M. A., Paul, J., and Van Arsdale, R. B. (2005). Space geodetic evidence for rapid strain rates in the New Madrid seismic zone of central USA. *Nature*, *435*(7045), 1088–1090. https://doi.org/10.1038/nature03642

Wang, L. F., Hainzl, S., Mai, P. M. (2015). Quantifying slip balance in the earthquake cycle: Coseismic slip model constrained by interseismic coupling. *J. Geophys. Res.*: *Solid Earth*, *120*(12), 8383–8403. https://doi.org/10.1002/2015JB011987

Wang, L. F., Hainzl, S., and Mai, P. M. (2017). To which level did the 2010 M 8 8 Maule earthquake fill the pre-existing seismic gap?. *Geophys. J. Int.*, *211*(1), 498–511. https://doi.org/10.1093/gji/ggx304

Wang, M., Shen, Z. K., Niu, Z. J., Zhang, Z. S., Sun, H. R., Gan, W. J., Wang, Q., and Ren, Q. (2003). Contemporary crustal deformation of the Chinese continent and tectonic block model. *Sci. China Ser. D*: *Earth Sci.*, *46*(2), 25–40. https://doi.org/10.1360/03dz0003

Weldon, R. J., Fumal, T. E. and Biasi, G. P. (2004). Wrightwood and the earthquake cycle: what a long recurrence record tell us about faults work. *GSA Today*, *14*(9). https://doi.org/10.1130/1052–5173(2004)014<4:WATECW>2.0.CO;2

Weldon, R. J., Fumal, T. E., Biasi, G. P., and Scharer, K. M. (2005). Past and Future earthquakes on the San Andreas fault. *Science*, *308*(5724), 966–967. https://doi.org/10.1126/science.1111707

Wells, D. L., and Coppersmith, K. J. (1994). New empirical relationships among magnitude, rupture length, rupture width, rupture area, and surface displacement. *Bull. Seism. Soc. Am.*, *84*(4), 974–1002.

Zhang, P.-Z., Shen, Z. K., Wang, M., Gan, W. J., Bürgmann, R., Molnar, P., Wang, Q., Niu, Z. J., Sun, J. Z., … You, X. Z. (2004). Continuous deformation of the Tibetan Plateau from global positioning system data. *Geology*, *32*(9), 809–812. https://doi.org/10.1130/g20554.1

Zhang, P. Z., Molnar, P., Burchfiel, B. C., Royden, L., Wang, Y. P., Deng, Q. D., Song, F. M., Zhang, W. Q., and Jiao, D. C. (1988a). Bounds on the Holocene slip rate of the Haiyuan Fault, North-Central China. *Quatern. Res.*, *30*(2), 151–164. https://doi.org/10.1016/0033–5894(88)90020–8

Zhang, P. Z., Molnar, P., Zhang, W. Q., Deng, Q. D., Wang, Y. P., Burchfiel, B. C., Song, F. M., Royden, L., and Jiao, D. C. (1988b). Bounds on the average recurrence interval of major Earthquakes along the Haiyuan Fault In North-Central China. *Seism. Res. Lett.*, *59*(3), 81–89. https://doi.org/10.1785/gssrl.59.3.81

Zhang, P. Z., Min, W., Deng, Q. D., and Mao, F. Y. (2005). Paleoearthquake rupture behavior and recurrence of great earthquakes along the Haiyuan Fault, northwestern China. *Sci. China Ser. D*: *Earth Sci.*, *48*(3), 364–375. https://doi.org/10.1360/02yd0464

Zielke, O., Arrowsmith, J. R., Ludwig, L. G., and Akçiz, S. O. (2010). Slip in the 1857 and earlier large earthquakes along the Carrizo plain, San Andreas fault. *Science*, *327*(5969), 1119–1122. https://doi.org/10.1126/science.1182781

Zielke, O., Arrowsmith, J. R., Grant Ludwig, L., and Akciz, S. O. (2012). High-Resolution Topography-Derived Offsets along the 1857 Fort Tejon Earthquake Rupture Trace, San Andreas Fault. *Bull. Seism. Soc. Am.*, *102*(3), 1135–1154. https://doi.org/10.1785/0120110230